

Stress-strain Constitutive Relation of OSB under Axial Loading: An Experimental Investigation

Guo Chen,* and Bin He

The objective of this study was to establish the stress-strain empirical mode of oriented strand board (OSB) with random surfaces and oriented core 0° pattern (R/0°/R). The OSB specimens were loaded along the longitudinal (0°), diagonal (45°), and transverse (90°) directions of plates. The loading direction had a significant effect on the behavior of OSB. The OSB in compression exhibited high non-linear elastic behavior up to failure, while it expressed linear behavior when loaded in tension. Four types of failure modes under compression were included: end cracks between flakes, central cracks between flakes, diagonal shear failure, and surface folding. Most of the specimens in tension failed in tensile failure suddenly without plastic deformation. A refined empirical model was suggested and found to be in good agreement with the experimental data. The results provided useful information for modeling various structures containing OSB.

Keywords: Oriented strand board; Failure modes; Mechanical behavior; Empirical model

Contact information: College of Civil Engineering, Nanjing Forestry University, Nanjing 210037, China;

* *Corresponding author:* chenguo2009@126.com; chenguo@njfu.edu.cn

INTRODUCTION

With the increasing awareness of environmental protection, timber harvesting is strictly restricted in many countries (Beck *et al.* 2010). This forces the use of substitutes for plywood, which is made from large diameter logs. Oriented strand board (OSB) is mainly made from thin wood flakes sliced from small-diameter, fast-growing trees. Dried flakes are then mixed with wax and waterproof adhesive; then they are hot-pressed into multilayer panels (Lin *et al.* 2014; Mirski *et al.* 2016). Due to its superior strength, stiffness, workability, and competitive pricing, OSB is regarded as a promising alternative to wood-based structural panels. The most common uses of OSB for the past several decades are wall sheathing, subflooring, roof decking, webs for wood joists, and furniture production (Chen *et al.* 2015; Islam *et al.* 2015; Xiao *et al.* 2015; Jin *et al.* 2016).

Conventionally, wood strands are oriented in layers during the creation process. The surface strands are usually aligned in the length direction of the panel, thus giving the panel its primary strength along this axis (also referred to as the parallel direction or strong axis). However, the core layers are generally cross-aligned to the surface layer like plywood (Zhang *et al.* 1998; Painter *et al.* 2006; Akrami *et al.* 2014). Zhou *et al.* (1989) and Suzuki and Takeda (2000) reported that the mechanical performance of OSB determined in the parallel direction was higher than that of the values in other directions. Alldritt *et al.* (2014) came to a similar conclusion that a 24% increase in the shear modulus for the 0°/+45°/-45°/ to 45°/+45°/0°/ alignment when compared with the 0°/90°/0°/ alignment. McNatt *et al.* (1992) found that the face strand alignment increased the bending

strength and stiffness in the aligned direction. Chen *et al.* (2008) developed a numerical model to predict the bending stiffness of OSB panels and found that the contribution of the outer layers is much more than those close to the neutral layers.

In addition to experimental research, theoretical models have been developed to evaluate the performance of OSB. It is well known that wood quality is controlled by its growing conditions, such as water, nutrients, and sunlight, which will eventually affect the characteristics of the OSB produced. Wood is also regarded as a honeycomb structure characterized by a high degree of anisotropy at all levels of the anatomical organization, leading to the complexity of the stress-strain relation of wood (Chen *et al.* 2011). Therefore, it is urgently necessary to determine the performance of the OSB, such as tensile strength, compressive strength, modulus of elasticity (MOE), Poisson's ratio, *etc.* Particularly, the stress-strain relation of OSB under uniaxial loading is key to modeling various structures that contain OSB. For simplification, the researchers typically have defined wood as an isotropic elastic material or orthotropic elastic-plastic materials (Morrissey *et al.* 2009; He *et al.* 2016). Saliklis and Mussen (2000) investigated the buckling behavior of simple supported OSB and suggested an elastic-plastic model incorporating geometric and material nonlinearities. Chen (2003) proposed a bilinear model of wood, and the stress state of wood was thought to be plastic. However, it could not completely reflect the true state of wood loaded in compression. Zhu *et al.* (2005) developed a model to simulate OSB webbed wood I-joists, assuming the OSB to be an elastic plastic material. Such an approach was shown to be reliable in comparison with the results of experimental investigation and numerical analysis. Racher *et al.* (2007) investigated the bending behavior of timber composite I-beams using a finite element method. The OSB was considered as orthotropic materials with transverse isotropy. Guan and Zhu (2009) proposed a three-dimensional nonlinear finite element model to evaluate the crack behavior of OSB webbed wood I-beams with openings. In the model, orthotropic elasticity was employed to model the linear elastic performance of both the tension and compression zones of OSB, but elasto-plasticity was used to simulate the compressive zones after stresses reached their yield point.

Although a non-linear relationship was developed to measure the response of OSB under uniaxial loading, previous studies did not take into account the descending stage of the stress-strain curve. This is not appropriate because the OSB can withstand a considerable load after reaching its ultimate carrying capacity. The objective of this study was to investigate the mechanical behavior and to establish the stress-strain constitutive relation of OSB subjected to vertical loading. The tests covered three in-plane board directions that were defined as longitudinal, transverse, and 45° diagonal.

EXPERIMENTAL

Materials

Oriented strand board (Hubei Bao Yuan Wood Industry Co., Ltd., Jingmen, China) is a multi-layer structure made from *Pinus tabulaeformis*, and the dimensions of strands were approximately 80 mm long × 20 mm wide × 0.8 mm thick. The strands were dried to a moisture content of 6% to 7%. After that, the strips were compressed and bonded together with phenol formaldehyde resin (95% wood, 5% wax and resin) (Yijiayi New Material Technology Co., Ltd., Yancheng, China). The strands in core layers were oriented along

the length of the panel and the two surface layers were oriented randomly. The internal bond strength, moisture content, and density of OSB was 0.43 MPa, 6.6%, and 580 kg/m³, respectively, which were provided by the manufacturer.

Sample preparation

The common dimensions of OSB panels available in the building material market were 2440 mm (length) × 1220 mm (width) × 9.5 mm (thickness). Clearly, this did not satisfy the demands of British standard BS EN 789 (2005). Firstly, the OSB panels chosen from different bundles were cut into strips 9.5 mm × 50 mm × 240 mm in size for compression testing, and 9.5 mm × 50 mm × 300 mm for tension testing. Note that the method of sampling had a great effect on the experimental results, and therefore should strictly comply with the British standard BS EN 1058 (1996). To fabricate specimens subjected to compression loads, each set of five OSB samples from the same angles, with respect to the major panel axis ($\alpha = 0^\circ, 45^\circ, \text{ and } 90^\circ$), were bonded together with outdoor epoxy adhesive (Yijiayi New Material Technology Co., Ltd., Yancheng, China), and the amount of adhesive used between two strips was 200 g/m² (Fig. 1).

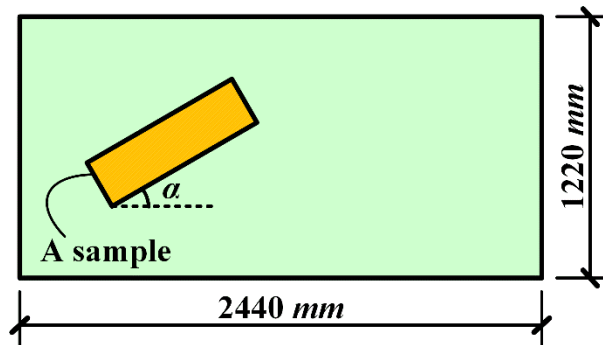


Fig. 1. A schematic diagram of cutting pattern used to fabricate specimens

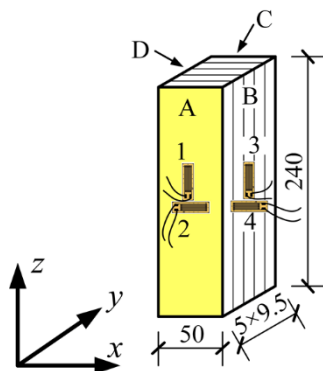


Fig. 2. Specimen in compression (Units: mm)

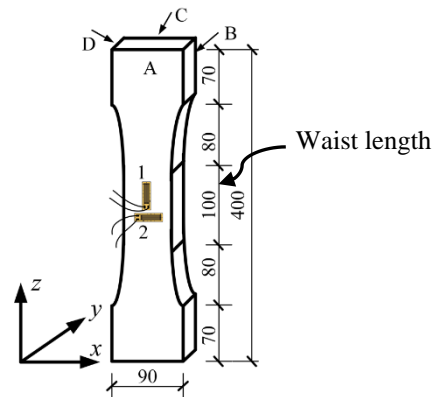


Fig. 3. Specimen in tension (Units: mm)

As soon as the gluing process was completed, the specimens were clamped with a heavy duty clamp. Finally, the finished specimens were stored in a conditioning room at 20 °C ± 2 °C and 65% ± 5% relative humidity for two weeks. Moreover, it is important to make sure that the failure of the samples was determined by material damage rather than

an adhesion connection between OSB strips. Given the effect of loading direction ($\alpha = 0^\circ$, 45° , and 90°) on the performance of the OSB, 20 identical specimens were tested for each group configuration.

As shown in Fig. 2, the four side faces of the specimens in compression were marked by a capital letter (A, B, C, or D) in a clockwise direction. For loading direction ($\alpha = 0^\circ$, 45° , and 90°), the specimens were named “st”, “xt”, and “ht”, respectively. To facilitate recording the failure phenomena conveniently, the facade of specimens in tension was numbered by letter “A”, and the back was assigned letter “C” (Fig. 3). The waist length of the specimens in tension was 100 mm. The “sc”, “xc”, and “hc” specimen series meant that the loading direction was 0° , 45° , and 90° , respectively.

Methods

The tests were conducted using an electro-hydraulic servo universal testing machine (Shenzhen Suns Technology Co., Ltd., Shenzhen, China) with a capacity of 100 kN with an accuracy of ± 0.1 kN. Eight strain gauges were bonded on each side face of the specimens in compression (Fig. 2). However, only four gauges were glued to the surface of the specimens in tension, two on side “A”, and two on side “C” (Fig. 4). It should be noted that the readings of strain gauges were reliable only in the elastic region, while in the plastic region the strain gauges lost contact with the surface of specimens and showed no value or inaccurate value due to a bonding problem (Motra *et al.* 2014). The extensometer recommended by BS EN 789 (2005) is suitable for measuring the change in length between two reference points. Thus, a highly accurate extensometer with an accuracy of ± 0.1 mm (NCS Testing Technology Co., Ltd., Beijing, China) was employed for measuring the deformations along the loading direction during the load-descending stage. However, the extensometer must be removed before reaching the ultimate load due to the possibility of destruction. All of the samples were loaded to failure under displacement control according to the provisions of BS EN 789 (2005). Load should be applied at a continuous rate of loading adjusted so that the maximum load is reached within (300 ± 120) s, and with a mean value of about 300s for a sample. To record the failure phenomenon of specimens in detail during the tests, the loading rate was 1.0 mm/min before the applied load reached to 60% of F_m (F_m is the maximum load), then dropped to 0.5 mm/min until the experiments were finished. All the experimental results were collected by a data acquisition system at a sampling frequency of 10 Hz. To eliminate systematic error and ensure that the machines were working reliably, pre-loading was needed before the formal experiments were done.

RESULTS AND DISCUSSION

Failure Modes of OSB in Compression

It was shown that the failure process of OSB loaded in compression was classified into three phases, which included the elastic stage, elastic-plastic stage, and descending stage. The specimens behaved elastically at the initial stage, and the deformation increased linearly with increased loading. At the end of the elastic stage, the first vertical hairline cracks parallel to the loading direction appeared near the steel head of the universal testing machine, rather than the top of specimens. This could have been viewed as a result of the horizontal hooping strengthening of the steel head.

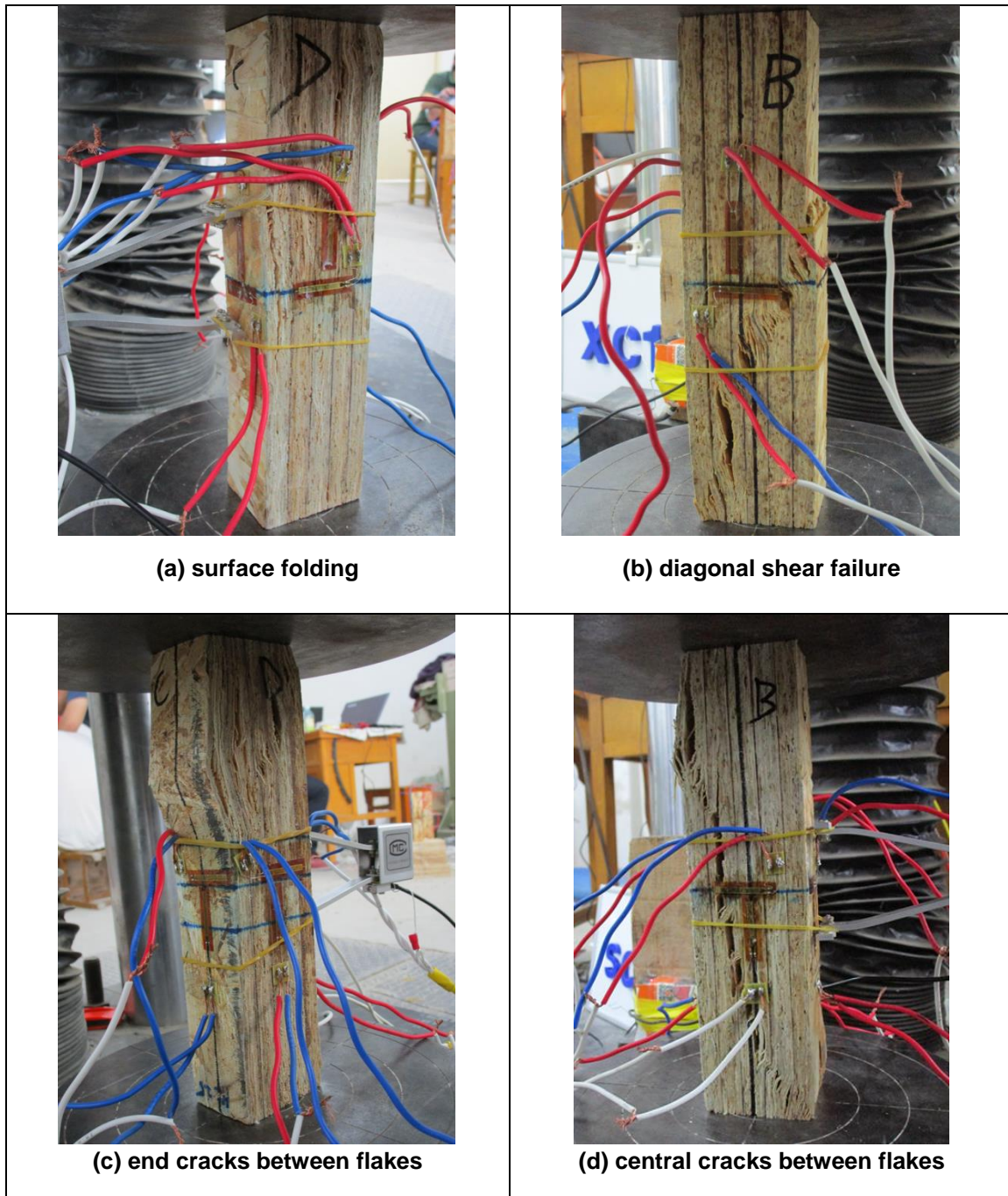


Fig. 4. Typical failure modes loaded in compression

In the subsequent elastic-plastic phase, cracks between wood flakes were generated at mid-height of the specimens accompanied by noises, and the width and the depth of the cracks expanded. As the compressive stress continued to increase, side “A” and side “C”, close to the mid-height of the specimen, a substantial uplift phenomenon appeared. The

vertical strain gauges damaged or lost contact with the surface of the specimens, while the others remained in good condition. After reaching the ultimate compressive strength, the load started to decline slowly. The cracks along the loading direction continued to widen and propagate rapidly towards the ends. The destruction happened with great deformation during failure, which showed good ductility with obvious signs of damage. The typical failure modes were shown graphically, as in Fig. 4. The folds and faults occurred on side “A” and side “C” for all of the specimens. Side “B” and side “D” were dominated by cracks between flakes, but the location and direction of the cracks were different. The longitudinal cracks for the “hc” group and “sc” group were located in the mid-height and the ends of the specimens, respectively, and diagonal cracks were investigated in the mid-height of the “xc” group. No adhesion failure occurred between wood strips.

It was clear that OSB subjected to compression loading exhibited linearly up to approximately 60% maximum stress, as shown in Fig. 5. Subsequently, the stress-strain displayed non-linear characteristics until the material reached its ultimate compressive stress. Afterwards, the stress degraded with increased strain until failure.

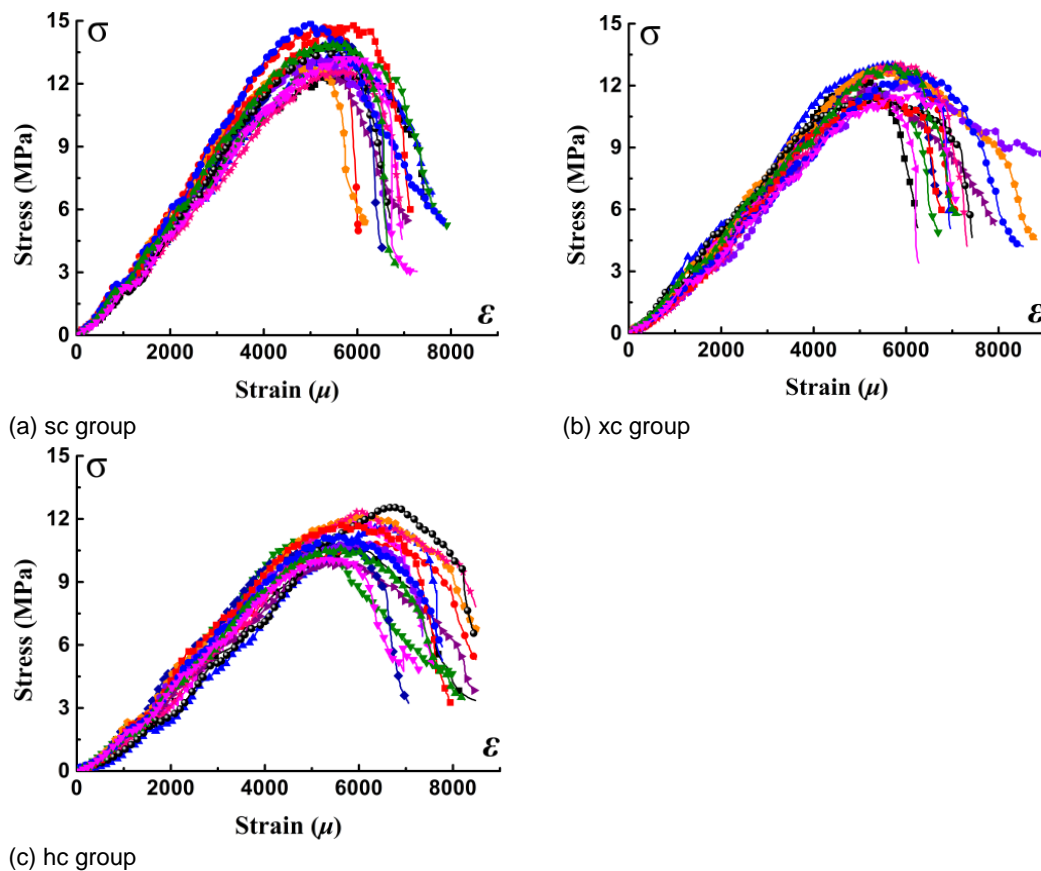


Fig. 5. Stress-strain relationship in compression

Failure modes of OSB in tension

Most of the specimens in tension failed suddenly, with no plastic deformation being apparent before fracture. As anticipated, the fracture shape depended on the angles with respect to the major panel axis. Most of the specimens failed within the parallel-sided

section of the waist length, as shown in Fig. 6. The crack directions were categorized as two types: (1) flat fracture surface that occurred in “ht” group specimens; and (2) cracking with a small angle relative to the horizontal that occurred in the rest of the specimens.

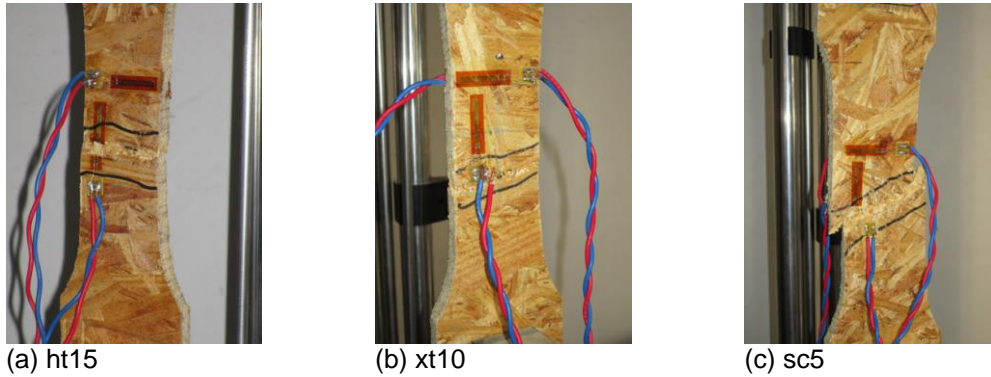


Fig. 6. Typical failure modes loaded in compression

As shown in Fig. 7, OSB in tension exhibited linear behavior up to failure and the ductility of specimens was poor without plastic deformation.

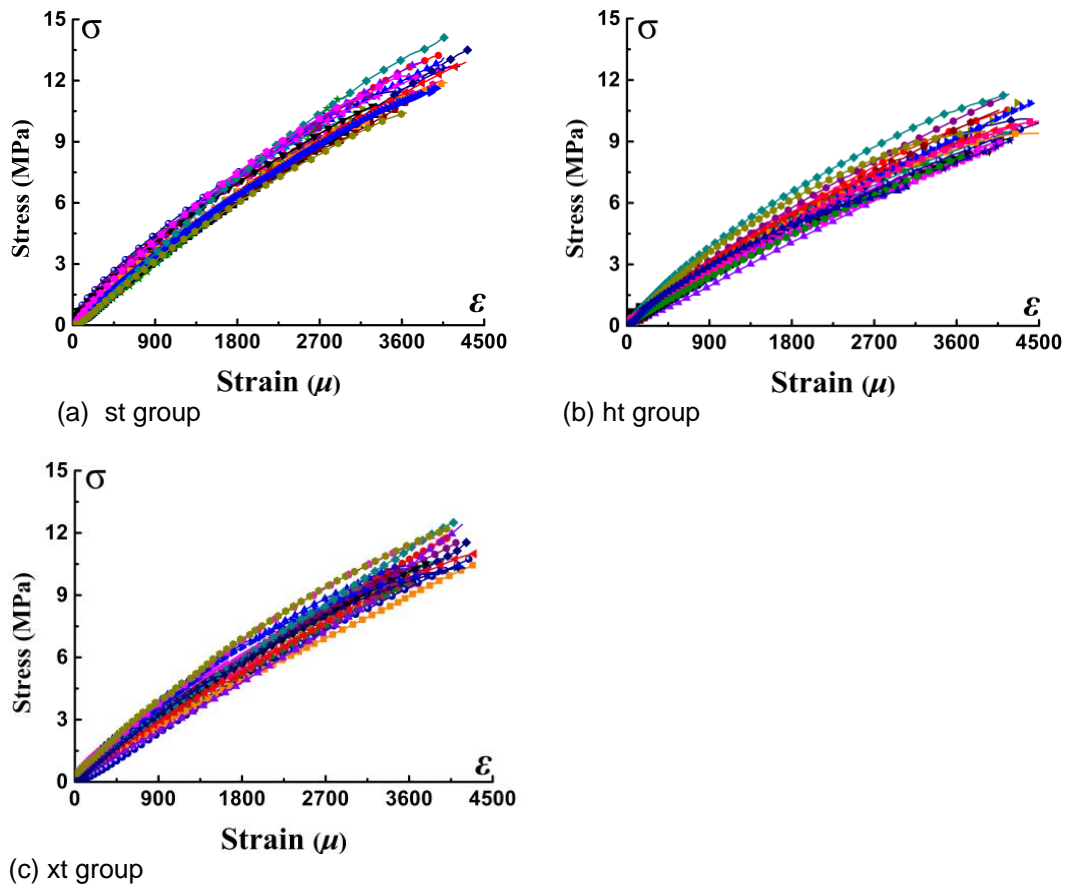


Fig. 7. Stress-strain relationship in tension

In compliance with BS EN 789 (2005), the data in Tables 1 and 2 were obtained. The specific data values of interest were: maximum carrying capacity (F_m), compressive strength (f_c), tensile strength (f_t), modulus of elasticity in compression (E_c), and modulus of elasticity in tension (E_t). It was evident that the angles relative to the longitudinal panel had great influence on the mechanical performance of OSB. When the angle increased, the modulus of elasticity and strength tended to decrease, but the effect on Poisson's ratio was negligible. The OSB with $\alpha = 0^\circ$ patterns produced the highest strength, followed by the $\alpha = 45^\circ$ patterns, and the $\alpha = 90^\circ$ patterns had the lowest. Akrami *et al.* (2014) and Alldritt *et al.* (2014) reached similar conclusions that the mechanical property of OSB determined in the parallel direction was higher than that of the values in the other directions.

Table 1. Performance of OSB in Compression

No.	F_m (kN)	f_c (MPa)	E_c (MPa)	No.	F_m (kN)	f_c (MPa)	E_c (MPa)	No.	F_m (kN)	f_c (MPa)	E_c (MPa)
sc1	29.92	12.4	3096	hc1	25.35	10.5	2703	xc1	30.02	12.2	2967
sc2	34.24	14.7	3329	hc2	27.89	10.8	2512	xc2	31.55	12.8	2811
sc3	32.93	13.5	3236	hc3	27.26	11.6	2549	xc3	30.26	13.0	2855
sc4	30.84	13.2	3065	hc4	28.59	11.0	2687	xc4	29.42	11.6	2936
sc5	32.01	12.9	3041	hc5	27.91	11.9	2568	xc5	27.51	11.1	2877
sc6	31.13	12.8	3401	hc6	23.79	9.9	2686	xc6	28.37	11.8	2628
sc7	34.20	14.0	3095	hc7	25.28	10.8	2729	xc7	31.13	12.9	3051
sc8	30.03	12.8	3531	hc8	29.61	12.1	2637	xc8	31.62	12.8	2779
sc9	33.15	13.3	3282	hc9	25.52	10.8	2484	xc9	32.91	13.3	2433
sc10	30.85	12.6	2983	hc10	29.94	12.4	2605	xc10	32.25	13.1	2946
sc11	31.80	13.8	3520	hc11	29.58	12.6	2461	xc11	29.01	11.4	2855
sc12	35.11	14.8	3093	hc12	28.09	11.7	2645	xc12	28.29	11.5	2887
sc13	35.77	14.9	3566	hc13	27.56	11.2	2552	xc13	29.66	12.5	2530
sc14	33.79	14.1	3411	hc14	26.98	10.6	2443	xc14	32.39	12.9	2631
sc15	31.81	13.4	3264	hc15	26.31	10.1	2379	xc15	29.94	11.6	2532
sc16	33.11	13.3	2991	hc16	32.75	13.6	2252	xc16	32.76	13.4	2831
sc17	34.77	14.2	3562	hc17	24.98	9.7	2203	xc17	28.23	11.5	2523
sc18	33.74	14.5	3411	hc18	29.85	12.4	2309	xc18	30.49	12.9	2557
sc19	33.81	13.3	3140	hc19	24.98	10.3	2198	xc19	35.41	14.6	2992
sc20	31.83	13.4	3049	hc20	29.09	11.7	2135	xc20	29.63	12.1	2762
Mean	32.74	13.6	3253	Mean	27.57	11.3	2487	Mean	30.54	12.5	2769
SD	1.70	0.75	202	SD	2.22	1.02	185	SD	1.96	0.88	184
COV	5.20%	5.52%	6.20%	COV	8.06%	9.03%	7.44%	COV	6.43%	7.04%	6.65%

Note: SD- Standard deviation, COV- Coefficient of variation

Table 2. Performance of OSB in Tension

No.	F_m (Kn)	f_t (MPa)	E_t (MPa)	No.	F_m (kN)	f_t (MPa)	E_t (MPa)	No.	F_m (kN)	f_t (MPa)	E_t (MPa)
st1	6.40	11.1	3056	ht1	5.67	9.2	2185	xt1	5.78	9.7	2630
st2	7.65	13.3	3299	ht2	6.56	10.6	2491	xt2	7.25	11.7	2944
st3	6.87	13.1	3231	ht3	5.59	9.3	2405	xt3	6.18	10.4	2856
st4	6.85	11.8	3106	ht4	5.76	9.7	2248	xt4	6.17	10.7	2695
st5	6.69	12.7	3089	ht5	5.42	9.1	2226	xt5	5.80	10.1	2673
st6	6.68	10.7	3351	ht6	5.88	10.9	2557	xt6	6.02	10.2	2812
st7	7.17	13.5	3128	ht7	6.04	10.1	2276	xt7	6.44	11.6	2741
st8	6.66	11.2	3046	ht8	5.69	10.5	2585	xt8	6.01	10.4	2840
st9	6.39	12.0	2973	ht9	5.02	8.3	2080	xt9	5.63	9.4	2523
st10	5.91	11.3	3247	ht10	5.17	8.4	2173	xt10	5.37	9.6	2618
st11	7.08	12.7	3001	ht11	6.12	10.0	2115	xt11	6.36	10.8	2559
st12	6.92	11.9	2908	ht12	5.34	9.4	2098	xt12	6.22	10.5	2439
st13	7.77	11.4	3472	ht13	6.35	11.1	2710	xt13	6.78	11.5	2803
st14	7.55	12.9	3358	ht14	5.92	8.9	2187	xt14	6.96	12.4	2973
st15	6.61	10.8	3252	ht15	5.70	8.6	2132	xt15	5.96	10.6	2783
st16	7.08	12.9	3001	ht16	5.93	9.9	2215	xt16	6.36	11.0	2559
st17	6.92	11.6	2908	ht17	5.84	11.0	2490	xt17	6.22	10.5	2534
st18	7.77	14.1	3472	ht18	6.61	11.3	2710	xt18	6.95	12.5	3067
st19	7.55	12.3	3358	ht19	5.81	9.0	2197	xt19	6.89	11.7	3021
st20	6.61	10.4	2852	ht20	5.70	9.5	2432	xt20	6.95	12.2	3167
Mean	6.96	12.1	3155	Mean	5.81	9.7	2326	Mean	6.32	10.9	2762
SD	0.49	1.0	186	SD	0.40	0.9	199	SD	0.50	0.9	196
COV	7.05%	8.34%	5.89%	COV	6.88%	9.16%	8.56%	COV	7.87%	8.25%	7.09%

Note: SD- Standard deviation, COV- Coefficient of variation

As shown in Tables 1 and 2, the OSB in compression had higher strength than that of OSB in tension. However, the difference of MOE in compression and tension was small, and only differed 3.0%, 6.5%, and 0.25% in the longitudinal, transverse, and 45° diagonal directions, respectively. To simplify the analysis, it can be considered that the MOE in tension and compression were equal. These results were similar to those obtained by Akrami *et al.* (2014), Alldritt *et al.* (2014), and Sumardi *et al.* (2007).

Poisson's Ratio

Under uniaxial stress conditions, the negative ratio of the lateral strain to the axial strain is called Poisson's ratio. For stresses within the elastic range, the Poisson's ratio is approximately constant. Equation 1 was used to calculate Poisson's ratio,

$$v = -\frac{\varepsilon_t}{\varepsilon_l} \quad (1)$$

where, ν is the Poisson's ratio, and ϵ_t and ϵ_l are the transverse strain (μ) and longitudinal or axial strain (μ), respectively. A previous study revealed that Poisson's ratio of different varieties of wood can be quite different (Ardalany *et al.* 2013). Based on the present work, the Poisson's ratios in tension of OSB were 0.24 and 0.17 for the major axis and minor axis, respectively. Thomas (2003) obtained similar results.

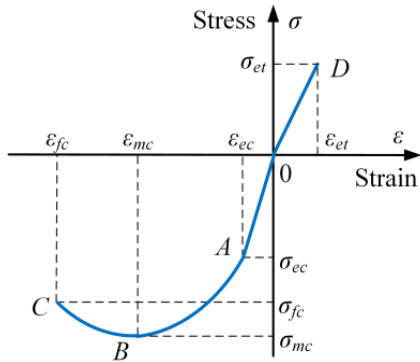


Fig. 8. Stress-strain model

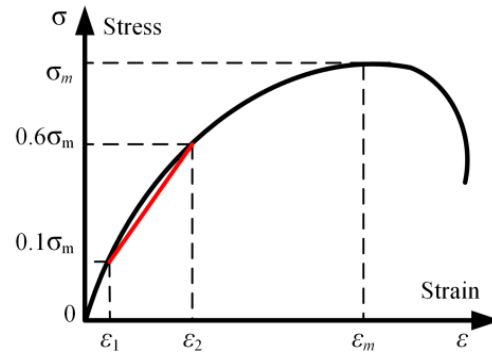


Fig. 9. Definition of MOE

Stress-strain Model

Based on the experimental results mentioned above, a refined model for the stress-strain relationship of OSB-loaded unidirectionally was proposed (Fig. 8). In this model, the failure process consisted of two stages, the tension stage and compression stage. Usually, the former is modeled by a straight line “OD”, and the latter is simulated by a straight line “OA” and a cubic polynomial curve “ABC”. As shown in Fig. 9, the modulus of elasticity (E_c and E_t) of specimens can be expressed as,

$$E_c = \frac{\sigma_{ec} - \sigma_1}{\epsilon_{ec} - \epsilon_1} \tag{2}$$

$$E_t = \frac{\sigma_{ec} - \sigma_1}{\epsilon_{ec} - \epsilon_1} \tag{3}$$

$$\sigma_1 = \frac{0.1F_m}{A} \tag{4}$$

$$\sigma_{ec} = \frac{0.6F_m}{A} \tag{5}$$

where $(\sigma_{ec} - \sigma_1)$ is the increment of stress on the straight-line portion of the strain-stress curve, $(\epsilon_{ec} - \epsilon_1)$ is the increment of strain corresponding to $(\sigma_{ec} - \sigma_1)$, A is the cross-sectional area of specimens (mm^2).

Zhu *et al.* (2005) suggested that 60% of the ultimate stress can be used as the initial yield stress for all loading directions. The variable ϵ_{mc} is the compressive strain (μ) corresponding to F_m (kN) (limit of load capacity). After reaching the ultimate compressive stress, the load began to decline gradually. It is generally believed that the specimen failed eventually, once the load drops to 80% F_m (Zheng *et al.* 2015). At this time, the compressive strain is defined as failure strain (ϵ_{fc}), and ϵ_{et} is the ultimate tensile strain,

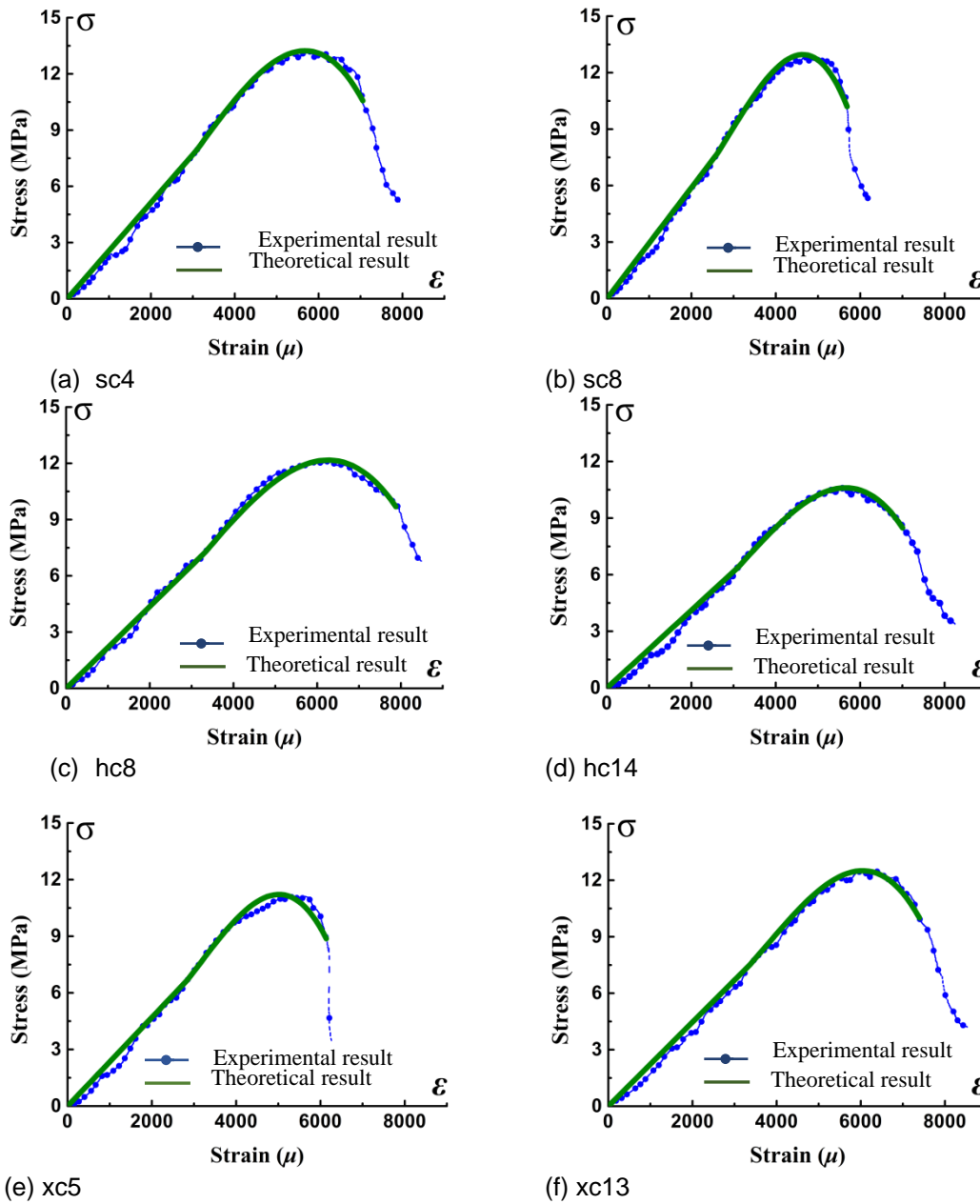


Fig. 10. Comparison of experimental result and theoretical result

$$\sigma(\varepsilon) = \begin{cases} E_c \varepsilon & \varepsilon_{ec} \leq \varepsilon \leq 0 \\ a\varepsilon^3 + b\varepsilon^2 + c\varepsilon + d & \varepsilon_{fc} \leq \varepsilon \leq \varepsilon_{ec} \\ E_r \varepsilon & 0 \leq \varepsilon \leq \varepsilon_{et} \end{cases} \quad (6)$$

where, a , b , c , and d are constants determined by the boundary compatibility conditions. Substituting the experimental data of stress and strain of OSB in compression, at points

$(0.6 \sigma_m, \varepsilon_{ec})$, $(1.0 \sigma_m, \varepsilon_{mc})$, and $(0.8 \sigma_m, \varepsilon_{fc})$ on the curve into Eq. 6, three equations containing parameters a , b , c , and d can be expressed according to the equation below.

$$\begin{cases} \sigma_{ec} = a\varepsilon_{ec}^3 + b\varepsilon_{ec}^2 + c\varepsilon_{ec} + d \\ \sigma_{mc} = a\varepsilon_{mc}^3 + b\varepsilon_{mc}^2 + c\varepsilon_{mc} + d \\ \sigma_{fc} = a\varepsilon_{fc}^3 + b\varepsilon_{fc}^2 + c\varepsilon_{fc} + d \end{cases} \quad (7)$$

Meanwhile, a smooth transition was proposed at the end points of curve “ABC” and line “OA”, which indicated the slope of the tangent to curve at the point $(\varepsilon_{ec}, \sigma_{ec})$ was equal to the slope of line (E_c) .

$$\sigma' \Big|_{\varepsilon=\varepsilon_{ec}} = 3a\varepsilon_{ec}^2 + 2b\varepsilon_{ec} + c = E_c \quad (8)$$

The parameters a , b , c , and d , with respect to the measured curves of specimens, can be obtained by solving Eqs. 7 and 8. As shown in Fig. 10, the results obtained by the theoretical models were in good agreement with the experimental results. This indicated that the model of uniaxial stress-strain relationship proposed above was reasonable.

CONCLUSIONS

1. Oriented strand board is a highly orthotropic material due to the inconsistent arrangement of wood flakes along both longitudinal and transverse directions. The flake orientation offered relatively higher mechanical properties in the longitudinal direction of OSB. Based on the results, the MOE of OSB samples in tension were found to be equal to that of in compression. The Poisson's ratios in tension of OSB were 0.24 and 0.17 for the major axis and minor axis, respectively.
2. The OSB subjected to compressive loading behaved elastically at the initial stage, followed by plastic deformation up to ultimate strength. After that, the load began to slowly drop until failure. There are four typical failure modes: end cracks, central cracks between flakes, diagonal shear failure, and surface folding.
3. The specimens in tension exhibited linear behavior until failure and failed suddenly without apparent plastic deformation before fracture. In addition, most of the specimens failed within the parallel-sided section of the waist length.
4. Considering the decline segments after peak value, a nonlinear empirical model for OSB was developed, and the results obtained from the theoretical models were in good agreement with the experimental results. The model has the capability to predict the mechanical behavior of various structures that contain OSB.
5. Only a few of specimens were tested in this paper, but there are a large number of factors that affect the properties of the OSB, such as tree species, processing technology, and so on. Therefore, further research is needed for a better understanding of the subject.

ACKNOWLEDGMENTS

The material presented in this paper is based upon work supported by the National Natural Science Foundation of China under Grant No. 51408312, the Natural Science Foundation of Jiangsu Province under Grant No. BK20130982, and a Project Funded by the Priority Academic Program Development of Jiangsu Higher Education Institutions (PAPD). Any opinions, findings, and conclusions or recommendations expressed in this material are those of the writer(s) and do not necessarily reflect the views of the foundations.

REFERENCES CITED

- Akrami, A., Barbu, M. C., and Fruehwald, A. (2014). "Characterization of properties of oriented strand boards from beech and poplar," *European Journal of Wood and Wood Products* 72, 393-398. DOI: 10.1007/s00107-014-0793-9
- Alldritt, K., Sinha, A., and Miller, T. H. (2014). "Designing a strand orientation pattern for improved shear properties of oriented strand board," *Journal of Materials in Civil Engineering* 26, 0401-4022. DOI: 10.1061/(ASCE)MT.1943-5533.0001033
- Ardalany, M., Fragiacom, M., Moss, P., and Deam, B. (2013). "An analytical model for design of reinforcement around holes in laminated veneer lumber (LVL) beams," *Materials and Structures* 46, 1811-1831. DOI: 10.1617/s11527-013-0019-3
- Beck, K., Cloutier, A., Salenikov, A., and Beauregard, R. (2010). "Comparison of mechanical properties of oriented strand board made from trembling aspen and paper birch," *European Journal of Wood and Wood Products* 68, 27-33. DOI: 10.1007/s00107-009-0350-0
- BS EN 789 (2005). "Timber structures – Test methods-Determination of mechanical properties of wood based panels," British Standards Organization, London, UK.
- BS EN 1058 (1996). "Wood-based panels – Determination of characteristic values of mechanical properties and density," British Standards Organization, London, UK.
- Chen, G., Li, H. T., Zhou, T., Li, C. L., Song, Y. Q., and Xu, R. (2015). "Experimental evaluation on mechanical performance of osb webbed parallel strand bamboo I-joist with holes in the web," *Construction and Building Materials* 101, 91-98. DOI: 10.1016/j.conbuildmat.2015.10.041
- Chen, S., Fang, L., Liu, X., and Wellwood, R. (2008). "Effect of mat structure on modulus of elasticity of oriented strandboard," *Wood Science and Technology* 42, 197-210. DOI: 10.1007/s00226-007-0167-0
- Chen, Y. X. (2003). *Flexural Analysis and Design of Timber Strengthened with High Strength Composites*, Master's Thesis, Rutgers University, New Brunswick, NJ, USA.
- Chen, Z. Y., Zhu, E. C., and Pan, J. L. (2011). "Numerical simulation of mechanical behaviour of wood under complex stress," *Chinese Journal of Computational Mechanics* 4, 629-634. DOI:10.7511/jslx201104024.
- Guan, Z. W., and Zhu, E. C. (2009). "Finite element modelling of anisotropic elasto-plastic timber composite beams with openings," *Engineering Structures* 31, 394-403. DOI: 10.1016/j.engstruct.2008.09.007

- He, M. J., Zhang, J., Li, Z., and Li, M. L. (2016). "Production and mechanical performance of scrimber composite manufactured from poplar wood for structural applications," *Journal of Wood Science* 62, 1-12. DOI: 10.1007/s10086-016-1568-1
- Islam, M. S., Shahnewaz, M., and Alam, M. S. (2015). "Structural capacity of timber i-joint with flange notch: Experimental evaluation," *Construction and Building Materials* 79, 290-300. DOI: 10.1016/j.conbuildmat.2015.01.017
- Jin, J., Chen, S., and Wellwood, R. (2016). "Oriented strand board: Opportunities and potential products in China," *BioResources* 11(4), 10585-10603.
- Lin, C. H., Yang, T. H., Lai, W. J., and Lin, F. C. (2014). "Anisotropic physical and mechanical performance of PF-impregnated oriented strand board," *BioResources* 8(2), 1933-1945. DOI: 10.15376/biores.8.2.1933-1945
- Painter, G., Budman, H., and Pritzker, M. (2006). "Prediction of oriented strand board properties from mat formation and compression operating conditions. 2. MOE prediction and process optimization," *Wood Science and Technology* 40, 291-307. DOI: 10.1007/s00226-005-0050-9
- McNatt, J. D., Bach, L., and Wellwood, R. W. (1992). "Contribution of flake alignment to performance of strandboard," *Forest Products Journal* 42, 45-50.
- Mirski, R., Dziurka, D., and Derkowski, A. (2016). "Properties of oriented strand boards with external layers made of non-strand chips," *BioResources* 11(4), 8344-8354. DOI: 10.15376/biores.11.4.8344-8354
- Morrissey, G. C., Dinehart, D. W., and Dunn, W. G. (2009). "Wood i-joists with excessive web openings: An experimental and analytical investigation," *Journal of Structural Engineering* 135, 655-665. DOI: 10.1061/(ASCE)ST.1943-541X.0000013
- Motra, H. B., Hildebrand, J., and Dimmig-Osburg, A. (2014). "Assessment of strain measurement techniques to characterize mechanical properties of structural steel," *Engineering Science and Technology, an International Journal* 17, 260-269. DOI: 10.1016/j.jestch.2014.07.006
- Racher, P., Bocquet, J. F., and Bouchair, A. (2007). "Effect of web stiffness on the bending behaviour of timber composite i-beams," *Materials & Design* 28, 844-849. DOI: 10.1016/j.matdes.2005.10.019
- Saliklis, E. P., and Mussen, A. L. (2000). "Investigating the buckling behavior of OSB panels," *Wood and Fiber Science* 32, 259-268.
- Sumardi, I., Ono, K., and Suzuki, S. (2007). "Effect of board density and layer structure on the mechanical properties of bamboo oriented strandboard," *Journal of Wood Science* 53, 510-515. DOI: 10.1007/s10086-007-0893-9
- Suzuki, S., and Takeda, K. (2000). "Production and properties of Japanese oriented strand board I: Effect of strand length and orientation on strength properties of sugi oriented strand board," *Journal of Wood Science* 46, 289-295. DOI: 10.1007/BF00766219
- Thomas, W. H. (2003). "Poisson's ratios of an oriented strand board," *Wood Science and Technology* 37, 259-268. DOI: 10.1007/s00226-003-0171-y
- Xiao, Y., Li, Z., and Wang, R. (2015). "Lateral loading behaviors of lightweight wood-frame shear walls with ply-bamboo sheathing panels," *Journal of Structural Engineering* 141, B4014004-1-9. DOI: 10.1061/(ASCE)ST.1943-541X.0001033

- Zhang, M., Wong, E. D., Kawai, S., and Kwon, J. H. (1998). "Manufacture and properties of high-performance oriented strand board composite using thin strands," *Journal of Wood Science* 44, 191-197. DOI: 10.1007/BF00521962
- Zheng, W., Lu, W., Liu, W., Wang, L., and Ling, Z. (2015). "Experimental investigation of laterally loaded double-shear-nail connections used in midply wood shear walls," *Construction and Building Materials* 101, 761-771. DOI: 10.1016/j.conbuildmat.2015.10.100
- Zhou, D. (1989). "A study of oriented structural board made from hybrid poplar. Physical and mechanical properties of osb," *European Journal of Wood and Wood Products* 47, 405-407. DOI: 10.1007/BF02626522
- Zhu, E. C., Guan, Z. W., Rodd, P. D., and Pope, D. J. (2005). "Buckling of oriented strand board webbed wood i-joists," *Journal of Structural Engineering* 131, 1629-1636. DOI: 10.1061/(ASCE)0733-9445(2005)131:10(1629)

Article submitted: April 12, 2017; Peer review completed: June 29, 2017; Revised version received: June 30, 2017; Accepted: July 1, 2017; Published: July 11, 2017.
DOI: 10.15376/biores.12.3.6142-6156